Preprint
UCRL-JC-143307

Case A Binary Evolution

C. A. Nelson and P. P. Eggleton

This article was submitted to
Astronomical Society of the Pacific 113th Annual Meeting, St. Paul, Minnesota, July 13-18, 2001

March 28, 2001

U.S. Department of Energy

Lawrence
Livermore
National
Laboratory

TITLE
ASP Conference Series, Vol. **VOLUME**, **PUBLICATION YEAR**
EDITORS

Case A Binary Evolution

Cailin A. Nelson & Peter P. Eggleton

Institute of Geophysics and Planetary Physics L-413, LLNL, Livermore, CA, 94550

Abstract. We undertake a comparison of observed Algo-type binaries with a library of computed Case A binary evolution tracks. The library consists of 5500 binary tracks with various values of initial primary mass M_{10}, mass ratio q_0, and period P_0, designed to sample the phase-space of Case A binaries in the range $-0.10 \leq \log M_{10} \leq 1.7$. Each binary is evolved using a standard code with the assumption that both total mass and orbital angular momentum are conserved. This code follows the evolution of both stars until the point where contact or reverse mass transfer occurs. The resulting binary tracks show a rich variety of behaviour which we sort into several subclasses of Case A and Case B. We present the results of this classification, the final mass ratio and the fraction of time spent in Roche Lobe overflow for each binary system. The conservative assumption under which we created this library is expected to hold for a broad range of binaries, where both components have spectra in the range G0 to B1 and luminosity class III – V. We gather a list of relatively well-determined observed hot Algol-type binaries meeting this criterion, as well as a list of cooler Algol-type binaries where we expect significant dynamo-driven mass loss and angular momentum loss. We fit each observed binary to our library of tracks using a χ^2-minimizing procedure. We find that the hot Algols display overall acceptable χ^2, confirming the conservative assumption, while the cool Algols show much less acceptable χ^2 suggesting the need for more free parameters, such as mass and angular momentum loss.

1. Introduction

Many binary stars are observed to be undergoing Roche-lobe overflow (RLOF), which is recognised as being a natural response to the fact that, for a binary of given separation, there is a critical maximum radius, the Roche-lobe radius, that a star cannot exceed without losing mass to its companion. There are many sub-types of stars undergoing RLOF, but we concentrate here on those which, like the prototype Algol, consist of (i) a lobe-filling, mass-losing star that is substantially above the main sequence, and (ii) a component which underfills its Roche lobe, and is usually nearer to, though still larger than, the main sequence. We concentrate on those (Case A) with short initial periods, the lower and upper period depending on the primary mass.

It is not difficult to evolve theoretically pairs of stars with a given initial primary mass M_{10}, initial mass ratio q_0 and initial orbital period P_0, and follow them into, and beyond, the stage of RLOF. However, such evolution is certainly affected by assumptions regarding both mass loss and angular momentum loss from the system as a whole. As a zero-order model it is commonly supposed that both total mass and orbital angular momentum are conserved, and we have computed conservative evolution for a large number of binary initial parameters: $37 \times 10 \times 15$ models with various M_{10}, q_0 and P_0. Most of the periods considered are appropriate to Case A, but some correspond to Case B.

There is plenty of evidence, both direct and indirect, that mass loss and/or angular momentum loss takes place in at least some systems. If mass escapes from the system as stellar wind, then it will also carry angular momentum away. Mass loss is observed fairly directly both in cool stars, where it appears to be driven by dynamo activity in their convective envelopes, and in hot stars, where radiation pressure in spectral lines may be the main driving force. Mass loss is also clearly evident in many stars of supergiant luminosity, across the whole range of spectral types; but we do not consider supergiants here. However there is a broad range of spectra, from about G0 to perhaps B1 and luminosity class III – V, where there is rather little evidence of significant mass loss, and where the conservative assumption may therefore be reasonable. We test this by comparing a selection of observed 'hot Algols' (having both spectra in this range) with theoretical conservative models, using a χ^2 test. We find a reasonable agreement, especially if we exclude one system which is near the extreme of this temperature range. Comparing the same conservative models against some observed 'cool Algols' we find, as we expect, that the agreement is much poorer.

We have used a massively-parallel array, the Compaq Teracluster 2000 at LLNL, to evolve our data cube of models. This data cube covers the following ranges of initial primary mass M_{10} (in solar units), initial mass ratio, defined by

$$q_0 \equiv \frac{M_{10}}{M_{20}} > 1 \ , \tag{1}$$

and initial period P_0:

$$\log(M_{10}/M_\odot) = -0.10, -0.05, \ldots, 1.7 \ , \tag{2}$$

$$\log q_0 = 0.05, 0.10, \ldots, 0.5 \ , \tag{3}$$

$$\log(P_0/P_{ZAMS}) = 0.05, 0.1, \ldots, 0.75 \ . \tag{4}$$

Here P_{ZAMS}, a function of M_{10}, is the period at which the initially more massive component would just fill its Roche lobe on the zero-age main sequence. We used the approximation

$$P_{ZAMS} \approx \frac{0.19 M_{10}/M_\odot + 0.47 (M_{10}/M_\odot)^{2.33}}{1 + 1.18 (M_{10}/M_\odot)^2} \ \text{days.} \tag{5}$$

These initial periods cover Case A and a small part of Case B.

To evolve our theoretical binaries, we used the stellar evolution code most recently described by Pols et al. (1995), based on the code of Eggleton (1971), Eggleton (1972), Eggleton, Faulkner & Flannery (1973). For a full discussion of the assumptions, input physics and stop-conditions we refer the reader to Nelson & Eggleton (2000). We mention briefly that the evolution of a binary system was terminated when a) the age of the system exceeded 20 Gyr, b) the carbon-burning luminosity exceeded 1 $L_\odot$, indicating a supernova explosion was imminent, c) the radius of $*1$ exceeded the Roche-lobe radius by more then 10%, d) $*2$ reaced RLOF, or, finally, e) the code failed to converge.

In §2 we attempt to classify the results into a small number of sub-categories of Case A (and some analogues in Case B). In §3 we discuss our attempts to fit several observed semidetached systems (Algols) with the theoretical models. We give our conclusions in §4.

We emphasise that throughout this paper we use suffixes 1 and 2 consistently to refer to the components with the greater and smaller *initial* mass respectively. This may seem unfortunate since observers normally call the currently hotter (and normally more massive) component the 'primary', at least in Algol systems. This component is the descendant of the originally less massive star. We do not think it would be helpful to interchange the suffices at the points in evolution where the ordering of the temperatures changes.

2. Classification of Types of Evolution

We define here the six major subtypes of Case A evolution identified by Eggleton (2000), cases AD, AR, AS, AE, AL, AN. In addition, we define two rather more rare cases, AG and AB. Three of these subtypes (AD, AR, AS) lead to contact while both components are on the main sequence (MS). Two cases (AE, AG) reach contact with one or both components evolved past the terminal MS. After the initial episode of mass transfer from $*1$ to $*2$, the remaining three cases experience a period of separation followed either by reverse mass transfer at very small q (AB, AL) or the supernova of $*1$ (AN). Specifically, the six cases, are:

- AD – dynamic RLOF: this occurs in binaries with large q_0 and in binaries where the mass losing star ($*1$) has a deep convective envelope. Once RLOF begins, mass transfer quickly accelerates to the dynamic timescale of $*1$ which we assume to be less than a tenth of the thermal timescale.

- AR – rapid evolution to contact: this occurs in binaries with moderate to large q_0. In these cases $*2$ expands so rapidly in response to the onset of $*1$'s thermal-timescale RLOF that it fills its own Roche lobe before much mass is transferred. This probably leads to a contact binary of the W UMa type, although it can happen as easily for massive stars (provided q_0 is suitably large) as for the lower masses of typical W UMa systems. Case AR behaviour is illustrated in Figure 1.

- AS – slow evolution to contact: this occurs in binaries with small q_0 and small P_0. These binaries experience a short burst of thermal timescale mass transfer, followed by a long phase of nuclear timescale mass transfer, during which much mass is exchanged. The two stars come into contact slowly, but reach contact before either star has left the MS. The large

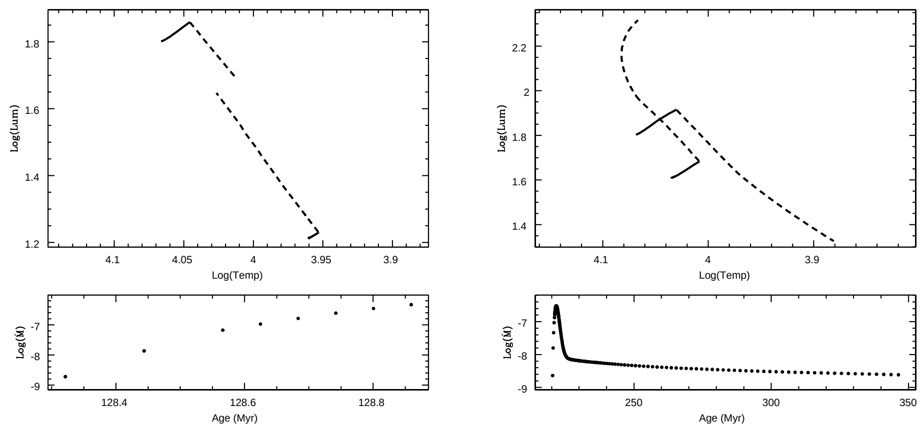

Figure 1. Case AR (left panel) and Case AS (right panel). In the top panels of this figure, and in Figures 2-3, we show the evolution of both stars in an HR diagram. The track for ∗1 is always the initially more luminous, ∗2 the initially less luminous. Solid lines indicate periods where the binary is separated, dashed lines indicate periods where ∗1 is transferring mass to ∗2. We mark any transitions to the Hertzsprung Gap as H, and transitions to the Giant Branch as G. The bottom panel shows the mass transfer rate in logarithmic units of $M_\odot$/yr for the period in time during which mass transfer occurs. The case AR binary has initial parameters $\log M_{10} = 0.45$, $\log q_0 = 0.15$ and $\log P_0/P_{\rm ZAMS} = 0.10$. The mass transfer rate rises rapidly to the thermal timescale and the two stars come into contact with a final mass ratio $\log q = 0.11$, still well above unity. The initial parameters of the Case AS binary are identical except that $\log P_0/P_{\rm ZAMS} = 0.20$. In this case, contact is avoided during the period of thermal scale mass transfer and a long period of nuclear timescale mass transfer follows. The run ends in contact with a final mass ratio, $\log q = -0.27$.

amount of mass transfer leads to a final mass ratio substantially below unity (typically $q \sim 0.4 - 0.6$), and with both stars substantially larger than their ZAMS radii. Case AS behaviour is illustrated in Figure 1. We note that while $*2$ always remains near the main-sequence band, $*1$ evolves to substantially cooler temperatures. This is a common configuration in observed Algol systems.

- AE – early overtaking: this occurs in binaries with q_0 near unity and moderate P_0. It occurs only in binaries with initial masses $2M_\odot \lesssim M_1 \lesssim 10M_\odot$. The mass transfer in this case is very similar to case AS. In case AE, however, $*2$ gains so much mass that its evolution is accelerated to the extent that $*2$ reaches the Hertzsprung Gap, HG, while $*1$ is still on the MS; the evolution of the initially less massive star, $*2$, has *overtaken* that of $*1$. We define the overtaking as *early* because it occurs with $*1$ still on the MS. Case AE behaviour is illustrated in Figure 2.

In most cases where contact is avoided while $*1$ is on the MS, $*1$ loses so much mass that it eventually shrinks inside its RL leaving only a compact core. A period of separation ensues which may then be followed by further RLOF of $*1$ or $*2$. These are the cases AL, AB and AN, described in more detail below. However, in our lower mass binaries ($M_{10} \leq 1.6M_\odot$) we see a few cases where contact is avoided while $*1$ is on the MS, but reached later on.

- AG – contact on giant branch: this occurs for $M_{10} \lesssim 1.6M_\odot$, and P_0 larger then those of AS/AE, but smaller then AL/AN. Contact is avoided while $*1$ is on the MS, but occurs when $*1$ reaches the giant branch, GB. At time of contact $*2$ is in the HG or on the GB as well. Case AG behaviour is illustrated in Figure 2.

Cases AL, AN are distinguished by whether or not $*1$ supernovas before $*2$ reaches RLOF. In practice, we assume a supernovae explosion to be iminent when $*1$ begins burning carbon.

- AL – late overtaking: this occurs in binaries with $M_{10} \lesssim 13M_\odot$ and moderate to large P_0. In these binaries, $*2$ reaches RLOF before $*1$ begins burning carbon. In many of the lower-mass AL cases, $*1$ has become a low mass remnant (WD or NS) which will never supernovae unless the (uncomputed) reverse mass transfer results in significant mass gain for $*1$. The evolution of $*2$ has *overtaken* the evolution of $*1$ in the sense that the initially more massive star is now shrunk inside its RL while the initially less massive star is undergoing RLOF. The overtaking is *late* because it occurs with $*1$ past the MS. Case AL behaviour is illustrated in Figure 3.

- AN – no overtaking: this occurs in higher mass binaries with moderate to large P_0. In these binaries $*1$ reaches carbon burning, indicating an imminent supernova, before $*2$ has reached RLOF. Case AN behaviour is illustrated in Figure 3.

In addition, we include one more class: the classic Case AB. In our context this is a subclass of case AL, where $*1$, after becoming a compact helium core

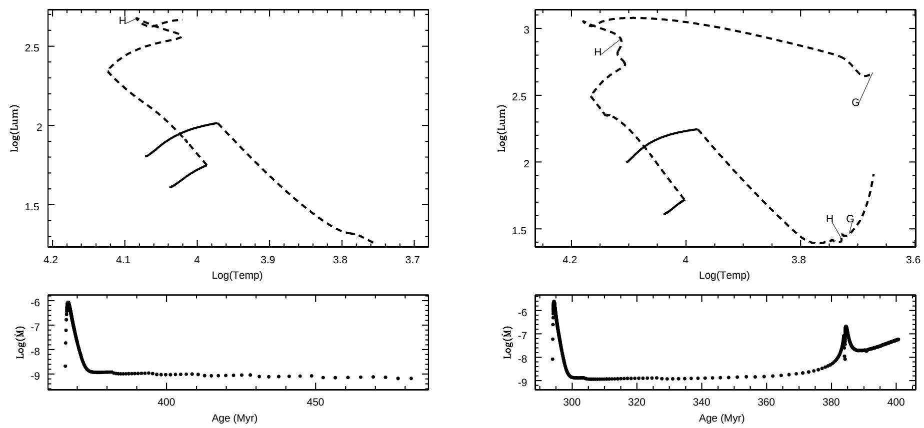

Figure 2. Case AE (left) and Case AG (right). The initial parameters of the case AE binary are $\log M_{10} = 0.45$, $\log q_0 = 0.05$ and $\log P_0/P_{\rm ZAMS} = 0.45$. $*2$ gains so much mass that it reaches the HG first. The initial parameters of the case AG binary are $\log M_{10} = 0.50$, $\log q_0 = 0.10$ and $\log P_0/P_{\rm ZAMS} = 0.55$.

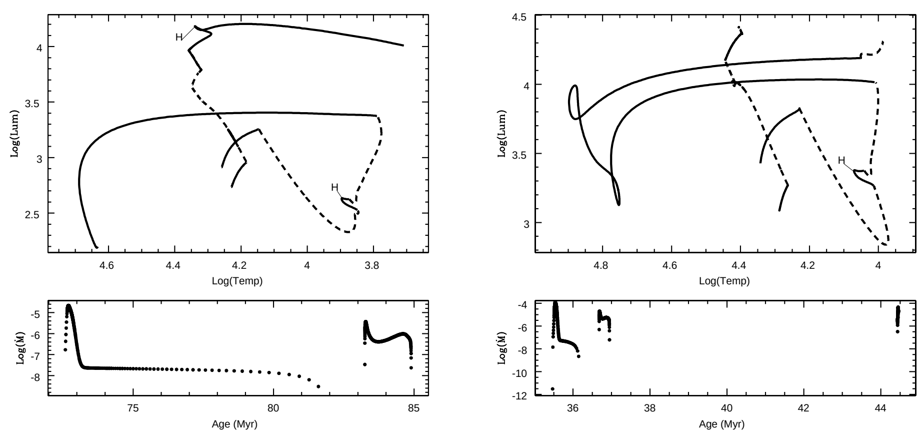

Figure 3. Case AL (left) and Case AN (right). The initial parameters of the Case AL binary are $\log M_{10} = 0.75$, $\log q_0 = 0.05$ and $\log P_0/P_{\rm ZAMS} = 0.60$. $*1$ loses so much mass it shrinks inside its RL and becomes a low mass helium burning core. The run ends as $*2$ crosses the HG and fills its RL at a very low mass ratio, $\log q = -1.07$. The initial parameters of the Case AN binary are $\log M_{10} = 1.15$, $\log q_0 = 0.05$ and $\log P_0/P_{\rm ZAMS} = 0.45$. After two periods of mass transfer, $*1$ becomes a helium star of mass $\log M_1 = 0.48$. As $*2$ evolves towards the terminal MS, $*1$ ignites carbon in the core, suggesting an imminent supernova explosion.

with a mass of $\sim 1 - 2M_\odot$, expands again and experiences a further period of RLOF.

- AB - this occurs in binaries with $6M_\odot \lesssim M_{10} \lesssim 11M_\odot$, at small mass ratios and in a narrow range of periods between cases AL and AN. During the second burst of mass transfer, $*1$ ignites helium. It shrinks inside its RL for awhile, becoming a compact helium star. It then expands again and experiences a third period of mass transfer. Although these binaries often fail to converge at some point during this third period of mass transfer, we suspect that it is followed by a period of separation and then reverse mass transfer, making this a subclass of AL rather then AN.

A plot showing which elements of our data cube reached which outcome may be found in Figure 9 of Nelson & Eggleton (2000). Some of the systems of longer P_0 are Case B rather than Case A. These are usually analogous to either AD, AR, AL or AN. Case BD is effectively the classical Late Case B, where $*1$ reaches the giant branch and acquires a deep convective envelope before RLOF begins; however it can also be an extreme initial mass ratio rather than a convective envelope which triggers dynamic mass transfer. Case B systems, or at least those which we have computed here, normally have fewer options than Case A because it is difficult for $*2$ to catch up with $*1$ when $*1$ has already reached the terminal main sequence before RLOF. However, as emphasised by De Greve (1990), it *is* possible for early Case B systems to show what we call here Case BL for late overtaking, with $*2$ evolving to fill its own Roche lobe while $*1$ has shrunk inside its own.

Further properties of our data cube including (i) the final mass ratio of each system and (ii) the fraction of time spent as a semidetached system have been illustrated and may also be found in Nelson & Eggleton (2000).

3. Comparison with Observed Systems

Many observed binaries are semidetached (Algols), and one might hope that they could be matched by some of the above theoretical models during their stage of RLOF. A significant study of this kind was conducted by De Greve (1993) in which non-conservative Case B binaries were fit to observed Algol systems.

We feel that although the kind of non-conservation modeled by De Greve (1993) may perhaps be appropriate for massive stars (O, and even early B), where radiation pressure may be an important agent in mass loss, it is not appropriate for mid-main sequence stars where, at least in single stars, very little mass loss is normally observed. At the other end of the main sequence, stellar winds are rather commonly observed, particularly in rapidly rotating G/K/M dwarfs (and even more so in giants). These winds probably do not carry off much mass (although see later), but they may be rich in angular momentum because of magnetic linkage to the parent star. We therefore think that conservative models may be reasonable for systems which are in the middle of the main sequence initially (say B1 to G0), and where the loser has not yet evolved to the red-giant region at spectra type $\sim$G or later. Following Popper (1980) we refer to these systems as 'hot Algols'. Unfortunately rather few of the Maxted

& Hilditch (1993) selection qualify as hot Algols in this sense, although two (U CrB and AF Gem) are on the border, with the cooler component having spectral type ~G0. We have therefore included a few more from the literature. Our selection of hot Algols is listed in Table 2, with references.

The observed parameters which we attempt to fit with our theoretical models are the six independent quantities $\log P$, $\log M_1$, $\log q$, $\log R_2$, $\log T_1$ and $\log T_2$. R_1 is not independent of these, since it is obtained from the *assumption* that $*1$ fills its Roche lobe, whose radius is determined by the first 3 parameters. L_1 and L_2 are similarly not independent of these 6 parameters. Our theoretical models have four independent parameters, $\log P_0$, $\log M_{10}$, $\log q_0$ and age.

For each system in Tables 2 and 3 we give three rows. The first gives the observational data from the literature, and the next the theoretical values from our data cube which minimize χ^2. The second row also includes the best-fit age, in units of Myr. The third row gives the zero-age values for the system which we infer from our best fit. We use mass-ratio q because this is usually obtained more directly from the observational data, whether spectroscopic or photometric, than either M_1 or M_2. We list observational errors (when available) in the first row for all quantities, but we list total errors (described below) in the second row only for those quantities that we actually fit.

In fitting observed stars to theoretical models, a χ^2 test seems appropriate. However, we have to modify the standard test in order to incorporate the fact that our theoretical models have an intrinsic 'graininess' because they have not been computed for a continuous range of input parameters, but only at the grid-points in our data cube. We therefore use a total error, σ, which is the sum in quadrature of the observational error, $\sigma_{\rm obs}$, and a 'theoretical error', $\sigma_{\rm th}$, representing the intrinsic graininess. For $\log P$, $\log M_1$ and $\log q$ we take $\sigma_{\rm th} = 0.05$, the initial spacing of our grid. For $\log R$ and $\log T$ we take the graininess to be the difference in these parameters between adjacent ZAMS models from the grid, centered on the mass of the observed binary. For example, for an observed star of mass $\log M = 1.02$ we take the theoretical error in the radius to be

$$\sigma_{\rm th,R}(\log M = 1.02) = R_{\rm ZAMS}(\log M = 1.05) - R_{\rm ZAMS}(\log M = 1.00)\ . \qquad (6)$$

We can then look in our data cube for the minimum value of

$$\chi^2 = \sum \frac{({\rm obs} - {\rm th})^2}{\sigma_{\rm obs}^2 + \sigma_{\rm th}^2}\ . \qquad (7)$$

We find that the best fit point picked by minimizing this χ^2 is insensitive to the exact definition of $\sigma_{\rm th}$. However, the magnitude of $\chi^2_{\rm min}$ depends directly on σ, so we have attempted a reasonable definition.

The hot Algols of Table 2 have a mean χ^2 of ~ 3. Since there are 2 degrees of freedom (6 observed parameters less 4 theoretical parameters), this value is rather more, but not enormously more, than is expected for a normal distribution of errors. The number of systems which we use is too small to provide a really convincing confirmation or refutation. The worst case, AF Gem, is very close to the lower temperature limit, where we suppose *a priori* that conservation might break down. If we reject AF Gem, we have a mean χ^2 of just 2.

Table 1. Hot Algols: observed parameters (first line), best fit parameters (second line) and ZAMS parameters (third line).

Star	log P	log $M_1/M_\odot$	σ_{M_1}	log q	σ_q	log $T_1(K)$	σ_{T_1}	log $T_2(K)$	σ_{T_2}	log $R_1/R_\odot$	σ_{R_1}	log $R_2/R_\odot$	σ_{R_2}	log $L_1/L_\odot$	σ_{L_1}	log $L_2/L_\odot$	σ_{L_2}	Age(Myr)	χ^2
TT Aur[8]	0.124	0.732	0.033	-0.176	0.010	4.366	0.030	4.296	0.030	0.632	0.010	0.691	0.011	3.310	0.030	3.710	0.030	...	...
...	0.149	0.769	0.066	-0.201	0.061	4.349	0.036	4.294	0.033	0.640	...	0.616	0.031	3.330	...	3.730	...	16	1.776
...	0.119	0.960	...	0.150	...	4.369	...	4.297	...	0.651	...	0.493	...	3.693	...	3.099	...	...	...
U CrB[4]	0.539	0.164	0.033	-0.430	0.033	3.767	0.016	4.170	0.009	0.694	0.009	0.436	0.011	1.420	0.060	2.610	0.120	...	...
...	0.547	0.159	0.066	-0.451	0.066	3.761	0.049	4.197	0.031	0.703	...	0.433	0.039	1.403	...	2.567	...	219	1.604
...	0.236	0.650	...	0.900	...	4.127	...	4.003	...	0.341	...	0.297	...	2.136	...	1.417	...	...	...
AF Gem[7]	0.096	0.063	0.016	-0.466	0.010	3.767	0.010	4.000	0.030	0.366	0.007	0.417	0.010	0.760	0.030	1.780	0.060	...	...
...	0.124	0.127	0.063	-0.312	0.061	3.776	0.027	4.033	0.027	0.414	...	0.436	0.039	0.593	...	1.527	...	636	11.294
...	0.096	0.400	...	0.900	...	4.029	...	3.979	...	0.264	...	0.169	...	1.619	...	0.503	...	...	...
u Her[5]	0.319	0.463	0.039	-0.409	0.033	4.064	0.030	4.300	0.030	0.643	0.029	0.763	0.033	2.490	0.060	3.690	0.060	...	...
...	0.330	0.497	0.069	-0.296	0.066	4.064	0.039	4.296	0.033	0.673	...	0.707	0.037	2.616	...	3.613	...	64	0.949
...	0.130	0.900	...	0.150	...	4.297	...	4.300	...	0.493	...	0.403	...	3.099	...	2.564	...	...	...
DM Per[6]	0.436	0.316	0.019	-0.647	0.011	3.930	0.010	4.360	0.030	0.677	0.009	0.663	0.009	2.000	0.060	3.390	0.100	...	...
...	0.459	0.313	0.063	-0.474	0.061	3.909	0.039	4.349	0.034	0.716	...	0.660	0.031	2.016	...	3.343	...	114	3.379
...	0.157	0.700	...	0.900	...	4.229	...	4.106	...	0.433	...	0.311	...	2.736	...	1.997	...	...	...
V Pup[9]	0.163	0.964	0.046	-0.377	0.069	4.360	0.060	4.430	0.040	0.734	0.034	0.799	0.030	3.560	0.300	4.300	0.160	...	...
...	0.156	0.927	0.069	-0.333	0.096	4.346	0.066	4.451	0.046	0.734	...	0.793	0.034	3.734	...	4.244	...	10	1.311
...	0.117	1.100	...	0.100	...	4.444	...	4.396	...	0.669	...	0.610	...	4.066	...	3.766	...	...	...
λ Tau[2,3]	0.597	0.976	0.009	-0.679	0.007	3.930	0.030	4.390	0.040	0.734	0.016	0.906	0.007	2.110	...	3.690	...	...	...
...	0.641	0.391	0.061	-0.639	0.060	3.933	0.049	4.349	0.049	0.919	...	0.903	0.030	2.391	...	3.557	...	99	2.919
...	0.264	0.750	...	0.900	...	4.369	...	4.129	...	0.463	...	0.341	...	2.913	...	2.136	...	...	...
Z Vul[1,8]	0.391	0.363	0.019	-0.367	0.039	3.966	0.030	4.366	0.040	0.663	0.019	0.673	0.019	2.070	0.060	3.300	0.160	...	...
...	0.397	0.376	0.063	-0.417	0.063	3.949	0.041	4.346	0.049	0.670	...	0.669	0.036	2.099	...	3.369	...	107	0.776
...	0.127	0.700	...	0.150	...	4.229	...	4.129	...	0.423	...	0.341	...	2.736	...	2.136	...	...	...

References. (1) Cester et al. (1977); (2) Fekel & Tomkin (1982); (3) Giuricin, Mardirossian & Mezzetti (1983) (4) Heintze & van Gent (1989); (5) Hilditch (1984); (6) Hilditch, Hill & Khalesseh (1992) (7) Maxted & Hilditch (1996); (8) Popper (1980); (9) Popper & Hill (1991);

Table 2. Cool Algols: observed parameters (first line), best fit parameters (second line) and ZAMS parameters (third line).

Star	log P	log $M_1/M_\odot$	σ_{M_1}	log q	σ_q	log $T_1(K)$	σ_{T_1}	log $T_2(K)$	σ_{T_2}	log $R_1/R_\odot$	σ_{R_1}	log $R_2/R_\odot$	σ_{R_2}	log $L_1/L_\odot$	σ_{L_1}	log $L_2/L_\odot$	σ_{L_2}	Age (Myr)	χ^2
S Cnc[14,8]	0.977	-0.638	0.036	-1.045	0.001	3.665	0.010	3.990	0.010	0.720	0.004	0.332	0.004	1.050	0.050	1.580	0.045	···	···
···	1.033	-0.605	0.062	-0.897	0.050	3.678	0.039	3.920	0.036	0.773	···	0.326	0.028	1.210	···	1.283	···	4182	14.447
···	-0.055	0.150	···	0.250	···	3.832	···	3.680	···	0.148	···	-0.144	···	0.580	···	-0.614	···	···	···
R CMa[11,12]	0.055	-0.775	0.049	-0.801	0.029	3.630	0.030	3.860	0.030	0.025	0.028	0.196	0.027	-0.410	0.160	0.760	0.180	···	···
···	0.152	-0.580	0.070	-0.653	0.058	3.676	0.048	3.782	0.039	0.192	···	0.214	0.077	0.041	···	0.508	···	19470	22.871
···	-0.319	0.000	···	0.350	···	3.751	···	3.569	···	-0.050	···	-0.386	···	-0.143	···	-1.544	···	···	···
RZ Cas[4]	0.077	-0.137	0.012	-0.480	0.010	3.672	0.020	3.934	0.005	0.288	0.007	0.223	0.008	0.160	0.080	1.120	0.020	···	···
···	0.109	-0.192	0.051	-0.412	0.051	3.674	0.043	3.884	0.036	0.296	···	0.233	0.028	0.239	···	0.954	···	3971	5.382
···	-0.105	0.150	···	0.200	···	3.832	···	3.718	···	0.148	···	-0.102	···	0.580	···	-0.379	···	···	···
TV Cas[3]	0.258	0.185	0.014	-0.393	0.008	3.720	0.040	4.020	0.020	0.517	0.007	0.498	0.008	0.860	0.170	2.030	0.090	···	···
···	0.265	0.134	0.052	-0.376	0.051	3.766	0.060	4.061	0.037	0.509	···	0.503	0.032	1.033	···	2.202	···	502	2.925
···	0.097	0.450	···	0.200	···	4.072	···	3.924	···	0.282	···	0.183	···	1.806	···	1.014	···	···	···
AS Eri[1,9]	0.426	-0.682	0.018	-0.968	0.012	3.720	0.030	3.930	0.030	0.340	0.023	0.196	0.016	0.470	···	1.060	···	···	···
···	0.542	-0.587	0.053	-0.791	0.051	3.676	0.048	3.880	0.048	0.451	···	0.186	0.029	0.558	···	0.848	···	3474	22.549
···	-0.005	0.150	···	0.500	···	3.832	···	3.569	···	0.148	···	-0.386	···	0.580	···	-1.544	···	···	···
TT Hya[8,14]	0.842	-0.229	0.132	-0.646	0.002	3.680	0.010	3.990	0.010	0.769	0.029	0.290	0.028	1.200	0.080	1.500	0.070	···	···
···	0.846	-0.270	0.141	-0.633	0.050	3.652	0.039	3.999	0.036	0.759	···	0.290	0.040	1.080	···	1.529	···	2262	0.718
···	0.226	0.200	···	0.100	···	3.879	···	3.802	···	0.167	···	0.090	···	0.803	···	0.339	···	···	···
AT Peg[5]	0.059	0.021	0.012	-0.325	0.008	3.690	0.017	3.920	0.005	0.332	0.006	0.270	0.006	0.380	0.070	1.190	0.030	···	···
···	0.090	-0.025	0.051	-0.289	0.051	3.712	0.031	3.913	0.036	0.341	···	0.266	0.027	0.483	···	1.139	···	2078	2.252
···	0.054	0.250	···	0.250	···	3.924	···	3.750	···	0.182	···	-0.050	···	1.014	···	-0.149	···	···	···
β Per[2,10]	0.457	-0.092	0.026	-0.663	0.010	3.650	0.028	4.100	0.017	0.544	0.012	0.462	0.006	0.630	···	2.190	···	···	···
···	0.554	-0.085	0.056	-0.537	0.051	3.692	0.047	4.018	0.036	0.626	···	0.466	0.031	0.973	···	1.959	···	1135	15.972
···	0.154	0.350	···	0.200	···	4.002	···	3.831	···	0.227	···	0.150	···	1.416	···	0.578	···	···	···
HU Tau[7]	0.313	0.057	0.011	-0.592	0.008	3.738	0.012	4.080	0.034	0.507	0.004	0.410	0.005	0.920	0.050	2.090	0.150	···	···
···	0.414	0.095	0.051	-0.405	0.051	3.733	0.028	4.078	0.045	0.594	···	0.419	0.031	1.075	···	2.102	···	515	18.311
···	0.247	0.450	···	0.250	···	4.072	···	3.878	···	0.282	···	0.169	···	1.806	···	0.803	···	···	···
TX Uma[6]	0.486	0.072	0.014	-0.606	0.010	3.740	0.016	4.110	0.010	0.627	0.007	0.451	0.006	1.170	0.065	2.300	0.040	···	···
···	0.525	0.096	0.052	-0.471	0.051	3.735	0.030	4.123	0.031	0.668	···	0.461	0.031	1.229	···	2.368	···	373	8.113
···	0.266	0.500	···	0.250	···	4.105	···	3.924	···	0.311	···	0.183	···	1.997	···	1.015	···	···	···

References. — (1) Cester et al. (1978); (2) Giuricin, Mardirossian & Mezzetti (1983); (3) Khalesseh & Hill (1992); (4) Maxted, Hill & Hilditch (1994a); (5) Maxted, Hill, & Hilditch (1994b); (6) Maxted, Hill, & Hilditch (1995a); (7) Maxted, Hill, & Hilditch (1995b); (8) Maxted & Hilditch (1996); (9) Popper (1973); (10) Richards, Mochnacki, & Bolton (1988); (11) Sarma, Vivekananda Rao & Abhyankar (1996); (12) Tomkin (1985); (13) Van Hamme & Wilson (1993)

When we turn to a selection of cooler Algols (Table 3) we find significantly larger χ^2 for many systems. This, we believe, is consistent with the view that they are less conservative, certainly of angular momentum (which is fairly readily removed by magnetic braking on something like a nuclear timescale), and perhaps also of mass. We do not normally think of stellar winds from cool dwarfs and subgiants as being strong enough to remove significant *mass*, and yet certain active (RS CVn) binaries show evidence to the contrary. Both Z Her Popper (1988) and to a lesser extent RW UMa (Popper 1988; Scaltriti et al. 1993) exhibit the phenomenon that the cooler, presumably more evolved, subgiant is the *less* massive star, despite the fact that it does not fill its Roche lobe. This suggests that mass loss by wind from the cooler star is already on the nuclear timescale of the star.

4. Conclusions

Case A RLOF, even when restricted to the classical 'conservative' model, shows a rich variety of behaviour, which we feel is often not emphasised enough. We identify 9 sub-classes, depending partly on whether the system evolves into contact (in 5 different ways) or reaches reverse RLOF (in 4 different ways). Further subdivision depends on the evolutionary states reached when contact or reverse RLOF occurs. We can expect even more subclasses when non-conservative processes are modeled, as will certainly be necessary for extremes of high-temperature and low-temperature systems.

For all but one of our selection of observed hot Algols we find an acceptable χ^2 when fitting the observed parameters to our library of conservative Case A binary tracks. It is encouraging to note that the worst outlier (AF Gem) lies near the lower boundary of the temperature range in which we expect the conservative assumption to hold. The next largest χ^2's come from two binaries with known third bodies (λ Tau, DM Per), which may act to remove angular momentum from the inner orbit.

Our selection of cool Algols shows significantly worse agreement between the observed systems and the conservative theoretical tracks, suggesting the need for more free parameters in the modelling, such as mass and angular momentum loss.

This data set of conservative Case A tracks has uses beyond an indiviual comparison of observed systems. With an estimate of the initial mass function and period distribution of binaries, it may be useful for population synthesis studies or for creating close binary-inclusive isochrones for stellar population studies. We hope to make these tracks available in early 2001 on the Institute of Geophysics and Planetary Physics web site http://www.llnl.gov/urp/IGPP.

This work was performed under the auspices of the U.S. Department of Energy by the University of California, Lawrence Livermore National Laboratory under contract No. W-7405-Eng-48.

References

Cester, B., Fedel, B., Giuricin, G., Mardirossian, F. & Pucillo, M. 1977, A&A, 61, 469

Cester, B., Fedel, B., Giuricin, G., Mardirossian, F. & Mezetti, F. 1978, A&A, 62, 291

De Greve, J. P. 1993, A&AS, 97, 527

De Greve, J. P. & Packet, W. 1990, A&A, 230, 97

Eggleton, P. P. 1971, MNRAS, 151, 351

Eggleton, P. P. 1972, MNRAS, 156, 361

Eggleton, P. P. 2000, in the Brian Warner Symposium, New Astronomy Reviews, 44, 111

Eggleton, P. P., Faulkner, J. & Flannery, B. P. 1973, A&A, 23, 325

Fekel, F. C. & Tomkin, J. 1982, ApJ, 263, 289

Giuricin, G., Mardirossian, F. & Mezzetti, M. 1983, ApJS, 52, 35

Heintze, J. R. W. & van Gent, R. H. 1988, in 'Algols', ed. Batten, A. H. Kluwer AP, p264

Hilditch, R. W. 1984, MNRAS, 211, 943

Hilditch, R. W., Hill, G. & Khalesseh, B. 1992, MNRAS, 254, 82

Khalesseh, B. & Hill, G. 1992, A&A, 257, 199

Maxted, P. F. L. & Hilditch, R. W. 1995, A&A, 301, 149

Maxted, P. F. L. & Hilditch, R. W. 1996 A&A, 311, 567

Maxted, P. F. L., Hill, G. & Hilditch, R. W. 1994a, A&A, 282, 821

Maxted, P. F. L., Hill, G. & Hilditch, R. W. 1994b, A&A, 285, 535

Maxted, P. F. L., Hill, G. & Hilditch, R. W. 1995a, A&A, 301, 135

Maxted, P. F. L., Hill, G. & Hilditch, R. W. 1995b, A&A, 301, 141

Nelson, C.A. & Eggleton, P.P., astro-ph 0009258.

Pols, O. R., et al. 1995, MNRAS, 274, 964.

Popper, D. M. 1973, ApJ, 185, 265

Popper, D. M. 1980, ARA&A, 18, 115

Popper, D. M. 1988, AJ, 96, 1040

Popper, D. M. & Hill, G. 1991, AJ, 101, 600

Richards, M. T., Mochnacki, S. W. & Bolton, C. T. 1988, AJ, 96, 326

Sarma, M. B. K., Vivekananda Rao, P. & Abhyankar, K. D. 1996, ApJ, 458, 37

Scaltriti, F., Busso, M., Ferrari-Toniolo, M., Origlia, L., Persi, P., Robberto, M. & Silvestro, G. 1993, MNRAS, 264, 5

Tomkin, J. 1985, ApJ, 297, 250

Van Hamme, W. & Wilson, R. E. 1993, MNRAS, 262, 220